

Ablation of $(\text{GeS}_2)_{0.3}(\text{Sb}_2\text{S}_3)_{0.7}$ Employing Nanosecond UV Laser

Petr Knotek^{1,3}, Jakub Navesnik¹, Milan Vlcek^{2,3} and Ladislav Tichy^{2,3}

¹University of Pardubice, Faculty of Chemical Technology, Studentska 573, 532 10 Pardubice, Czech Republic

²Institute of Macromolecular Chemistry, AS CR, Heyrovského sq. 2, 162 06 Prague, Czech Republic

³Present address: Joint Laboratory of Solid State Chemistry of Institute of Macromolecular Chemistry Academy of Sciences of Czech Republic, v.v.i., and University of Pardubice, Studentska 84, 532 10 Pardubice, Czech Republic

Keywords: Chalcogenide Glass, Ablation, UV Nanosecond Laser, Microlens.

Abstract: The interaction of $(\text{GeS}_2)_{0.3}(\text{Sb}_2\text{S}_3)_{0.7}$ glass and UV nanosecond laser has been described. The material was ablated and the dependencies of the most important parameters as number and energy of the pulses and repetition rate to the volume of the craters were correlated.

1 INTRODUCTION

Laser based fabrication technologies are widely used to prepare: thin films (PLD (Frumar et al., 2006)), optical waveguide (Bryce et al., 2004), convex or concave microlenses and microlens arrays (Lim et al., 2006); (Fritze et al., 1998) as the passive optical elements. The patterns are formed by the focusing laser energy in order to process materials at the microstructure (Hitz et al., 2012). Different types of laser operation (continuous or pulsed modes) enable to use proper combination of laser experimental set-up to studied material and demanding process. The absorption of photons can lead to excitation of electrons in target materials. If the energy is high enough, the energy transfer leads to the material release by thermal vaporization or by photochemical interactions (Hitz et al., 2012); (Knotek et al., 2012).

The influence of ultraviolet light (UVL) to the certain optical and physical behavior of the chalcogenide glasses and films has been previously studied. There were described the classical photo-induced effects as photo-darkening, photo-expansion and decrease of the refractive index (Bryce et al., 2004); (Messaddeq et al., 2001); (Marquez et al., 2009). The unique changes of behavior were accounted to the photo-induced structural changes in an amorphous state, reaction with surroundings as photo-oxidation or crystallization of the material (Messaddeq et al., 2001), (Bryce et al., 2004).

In this communication we focused on the interaction of UV pulsed laser with the bulk glassy $(\text{GeS}_2)_{0.3}(\text{Sb}_2\text{S}_3)_{0.7}$ material. Ge-Sb-S system, mainly

$(\text{GeS}_2)_x(\text{Sb}_2\text{S}_3)_{1-x}$ stoichiometric system, renewed attractiveness (Fatome et al., 2009); (Lin et al., 2012) for a high stability to the humid air, high linear and non-linear values of the refractive index and high glass forming and crystallization temperatures. We selected this chemical composition as chemically (stoichiometric system) and mechanically stable system (mean coordination number of the glass (CN=2.45) is close to the threshold value according Phillips model (Phillips, 1979)). The aim of this study was to examine interaction of nanosecond UV laser with $(\text{GeS}_2)_{0.3}(\text{Sb}_2\text{S}_3)_{0.7}$ glass and to determine some of the most important parameters as the pulse laser energy, the repetition rate and the number of pulses in relation to the modification of the sample.

2 EXPERIMENTAL

The glassy $(\text{GeS}_2)_{0.3}(\text{Sb}_2\text{S}_3)_{0.7}$ bulk was prepared by a direct synthesis from elements (5N purity) according procedure described elsewhere (Knotek and Tichy, 2012). The optically polished samples were illuminated under the air atmosphere through 5 nsec pulsed laser operating at a wavelength 213 nm in the laser ablation system LSX-213 G2 (CETAC, USA) with the maximum emitted energy 4.5 mJ per pulse.

The laser beam was focused onto the upper surface by means of an optical microscope objective to the spot with a diameter 25 μm . Two sets of illuminated spots were formed for each combination

Table 1: Material characteristics of the $(\text{GeS}_2)_{0.3}(\text{Sb}_2\text{S}_3)_{0.7}$ glass (E_{03} band gap energy, the average coordination number (CN)) and certain parameters which characterize the conditions of illumination: the wavelength (λ_{ill}) and photon energy ($h\nu_{\text{ph}}$), the pulse energy (E^{pulse}), the average emitted light intensity at repetition 20 Hz (I^{aver}), the corresponding penetration depth of the light (d_p), the area of the light spot on the sample (A), the effective volume ($V_{\text{eff}}=A*d_p$), where photons are adsorbed and the absorbed light power (P_A) during the pulse and average value.

E_{03}/CN^* (eV/-)	$\lambda_{\text{ill}}/h\nu_{\text{ph}}$ (nm/eV)	$E^{\text{pulse}}/I^{\text{aver}}$ (mJ/mW)	d_p (nm)	A (cm^2)	V_{eff} (cm^3)	$P_A^{\text{aver.}}/P_A^{\text{pulse}}$ ($\text{W}\cdot\text{cm}^{-3}$)
2.11/2.45	213/5.82	4.5/90	5	4.9×10^{-6}	2.5×10^{-12}	$3.7\times 10^{10}/3.7\times 10^{17}$

* $\text{CN} = 4x+3y+2(1-x-y)$ for $\text{Ge}_x\text{Sb}_y\text{S}_{1-x-y}$ (Philips, 1979)

of experimental parameters.

The chemical composition was verified using electron microprobe X-ray (EDX) analyses (Jeol JSM 5500-LV). In order to monitor surface and near-sub-surface states the penetration depth of electrons was adjusted to be at around 500 nm. The transmission was measured using a Perkin-Elmer Lambda 12 spectrophotometer.

Measurements with a digital holographic microscope (DHM) were realized by means of a DHMR1000 (Lyncée Tec, Switzerland) operating at 785 nm in a reflection configuration (Knotek et al., 2009).

3 RESULTS AND DISCUSSION

Certain material characteristics of the studied glass and the conditions of the samples illumination are summarized in Table 1 (see (Knotek and Tichy, 2012); (Knotek et al., 2010) for details of analysis). The UV photon energy was highly over-band gap energy ($E_{\text{ph}}=5.82$ eV $\gg E_{03}=2.11$ eV) and photons were absorbed in thin layer ($d_p=5$ nm). These conditions resulted to the high values of absorbed light power ($P_A^{\text{pulse}} = 4\times 10^{17}$ $\text{W}\cdot\text{cm}^{-3}$) followed by a destruction of the bonding system, photons energy conversion to the heat with low dissipation of the heat and vaporization of the material (Mendes, 2006).

There were tested three the most important parameters for laser-material interaction: the pulse laser energy (0.2 – 4.5 mJ per pulse denoted as series 1), the number of pulses (1 – 50 pulses - series 2) and the repetition rate (1 – 20 Hz - series 3). If not mentioned elsewhere, the typical conditions were 4.5 mJ per pulse, 20 Hz repetition rate, number of pulses 50 and 25 μm spot diameter.

Under all mentioned conditions, there were created craters after UV exposition of $(\text{GeS}_2)_{0.3}(\text{Sb}_2\text{S}_3)_{0.7}$ as summarized in Fig. 1a. The SEM details of craters “drilled” with the maximum energy (4.5 mJ) and 50 pulses with the repetition

rate 20 Hz and 1 pulse with 4.5 mJ energy are depicted in Fig. 1b and 1c, resp. All the craters were subsequently topographically analysed employing digital holographic microscope (DHM). The typical line-scans across the centre of the craters are illustrated in Fig. 2.

The diameter of the craters with maximal pulse energy was 95 – 100 μm with the depth 3.3 μm . The obtained craters were analyzed employing AFM software (Klapetek et al., 2011) to determine the

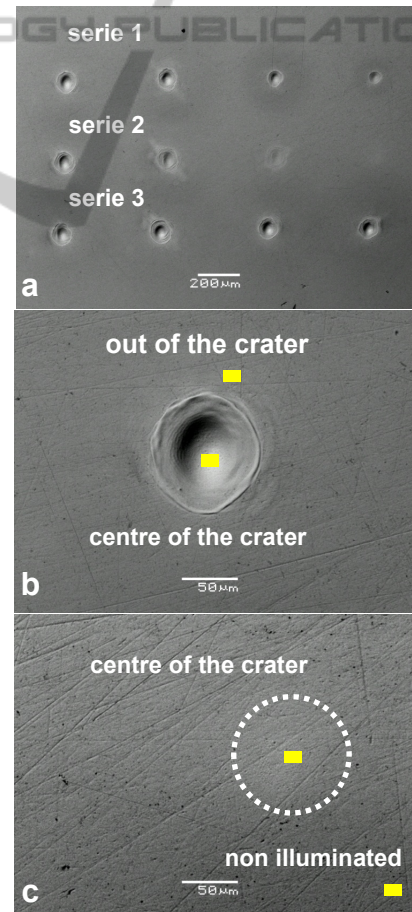


Figure 1: SEM images of ablated craters a) summarizing photo; b,c) details of the crater created by 50 pulses, 4.5 mJ per pulse, and by single 4.5 mJ pulse, resp.

volume of the crater as the parameter chosen for a crater characterization. The reproducibility of the process was checked by analysis of the six craters prepared under similar conditions of illumination (50 pulses, 4.5 mJ per pulse and 20 Hz repetition). The average volume was determined as $10\,600\ \mu\text{m}^3$ with standard error less than $300\ \mu\text{m}^3$ which seems to be reproducible values and the process.

The volume of the craters increased nonlinearly with the increase of the counts or the pulse energy (Fig. 3) independently on the way of supply of the cumulative energy. The line-scans detected the differences in the shape of the craters. If the craters were formed by low pulse energy (0.2 mJ per pulse), the profile is “V-shaped”, however with the higher pulse energy (>0.6 mJ per pulse) the profile is “U-shaped”. The craters formed with low energy pulse (0.2 mJ) could be used as an element of the microlens array. The curvature (R) of the circle formed when passes through the three points (two on the basal plane and one at a maximum of microlenses) equals to: $R = (d^2 + r^2)/2d = (2.7^2 + (54/2)^2)/(2 \times 2.7) = 136\ \mu\text{m}$, where d is the depth of the microlens and r is the radius of the basal plane. This value seems to be well comparable to R values for the microlens in oxide ($R \approx 150\ \mu\text{m}$) or in chalcogenide ($R \approx 170\ \mu\text{m}$) glasses (Beadie et al., 1998); (Huang et al., 2008); (Knotek and Tichy, 2012). The micro-scratches, as the consequence of the polishing of the bulk material, were partly smoothed even after single pulse (marked spot area on Fig. 1c).

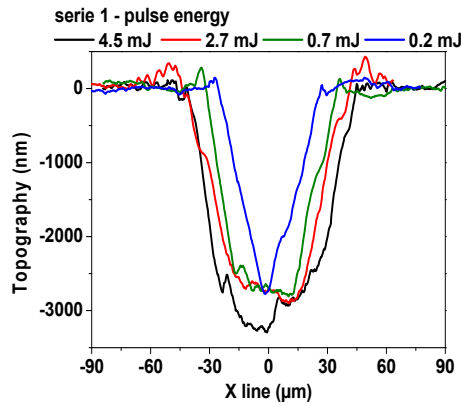


Figure 2: The line-scans of the craters of the serie 1 (the energy of the pulses in range 4.5 – 0.2 mJ, 50 pulses -see text).

The volume of the craters are independent on the repetition rate in the range 5 – 20 Hz (see Fig. 3, blue line); whereas the volume slightly decrease ($<15\%$) for the lowest repetition rate (1 Hz). The

low sensitivity of the volume to the repetition rate could be caused by the nanosecond time period for energy of UV photons to transfer to the heat and to vaporize the material during the pulse.

The chemical composition and its changes after the process of illumination were tested by EDX analysis on the areas denoted on Fig. 1 as the yellow rectangles. From the EDX analyses we found a constant ratio of small and rather broad K_{O} line at around 0.55 eV and L_{Ge} line at around 1.2 eV ($I_{\text{Ge}}/I_{\text{O}} \approx 3.6$) for the non-illuminated sample and for the sample illuminated for 1 pulse with $P_{\text{A}}^{\text{pulse}} = 1.6 \times 10^{16}\ \text{W}\cdot\text{cm}^{-3}$. Hence we suppose that within the sensitivity of EDX analyses there is practically no serious indication of photo-oxidation. We believe that this is an acceptable result because from kinetics limits photo-oxidation requires a time > 5 nsec even for the photons with an energy above 5 eV. On the other hand, the partial oxidation is evident in EDX comparing the centre of the crater and the deposit after ablation near the crater formed by 50 pulses (for location see Fig 1b) with non-illuminated glassy bulk as an increase of the broad O band near 0.55 eV ($I_{\text{Ge}}/I_{\text{O}} = 2.6$ and 2.1 for the crater center and the deposit out of the crater, resp.).

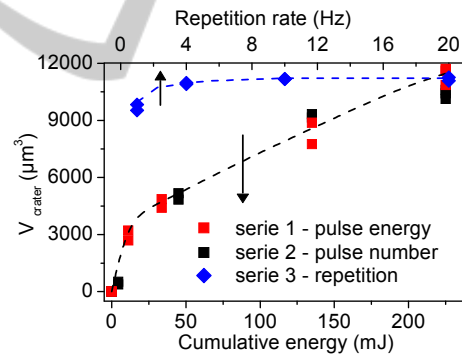


Figure 3: The dependences of the crater volume on the experimental conditions.

As mentioned in Introduction, the UV photo-induced expansion of the material is described in the literature. In present experiments the “gentle” exposition condition was realized by increasing of the diameter of the illuminated spot to the $200\ \mu\text{m}$ and minimal pulse energy 0.2 mJ ($P_{\text{A}}^{\text{pulse}} = 2.5 \times 10^{14}\ \text{W}\cdot\text{cm}^{-3}$). The material was still ablated after 5 pulses even under the low energy conditions (0.2 mJ) however the single pulse led to the elevation of the material (Fig. 5). Observed expansion of the material by 50 nm had to be connected with thermal-effect. UV photons can penetrate less than 5 nm which is

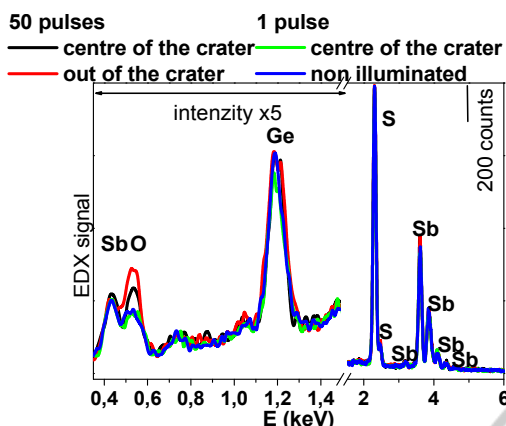


Figure 4: The EDX spectra of the samples, for location of analysis see Fig. 1 and the text.

too small depth to expand the material by 50 nm. Hence the heat should be dissipated deeper into the bulk.

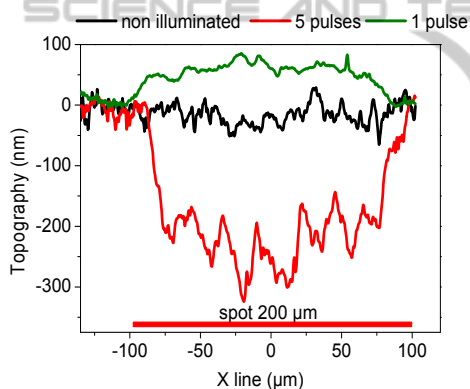


Figure 5: The line-scans of non-illuminated material, material after 5 and single pulse (200 μm diameter of the spot, pulse energy 0.2 mJ)

4 CONCLUSIONS

- The interaction of the 213 nm UV nanosecond laser with chalcogenide glass $(\text{GeS}_2)_{0.3}(\text{Sb}_2\text{S}_3)_{0.7}$ has been described;
- Influence of the most important parameters as energy of the pulse, number of pulses and repetition rate on the volume of the craters has been described;
- The shape of the craters is dependent on the condition of illumination and at low energy pulses created craters could be used for formation of microlens array;
- Future work will be focused on the structural changes of the material and analysis of the ablated

material.

ACKNOWLEDGEMENTS

The authors acknowledge financial support from the project Grant Agency of the Czech Rep. (GPP108/12/P044). We are indebted to Dr. M. Kincl for technical assistance.

REFERENCES

- Beadie, G., Rabinovich, W. S., Sanghera, J. & Aggarwal, I. 1998. Fabrication of microlenses in bulk chalcogenide glass. *Opt. Commun.*, 152, 215-220.
- Bryce, R. M., Nguyen, H. T., Nakeeran, et al. 2004. Direct UV patterning of waveguide devices in As_2Se_3 thin films. *J. Vac. Sci. Technol. A*, 22, 1044-1047.
- Fritze, M., Stern, M. B. & Wyatt, P. W. 1998. Laser-fabricated glass microlens arrays. *Opt. Lett.*, 23, 141-143.
- Frumar, M., Frumarova, B., Nemeč, P., Wagner, T., Jedelsky, J. & Hrdlicka, M. 2006. Thin chalcogenide films prepared by pulsed laser deposition - new amorphous materials applicable in optoelectronics and chemical sensors. *J. Non-Cryst. Solids*, 352, 544-561.
- Hitz, B., Ewing, J. & Hecht, J. 2012. *Introduction to Laser Technology*, New York (USA), Wiley-IEEE Press.
- Huang, Y., Liu, R., Lai, J. J. & Yi, X. J. 2008. Design and fabrication of a negative microlens array. *Opt. Laser Technol.*, 40, 1047-1050.
- Klapetek, P., Nečas, D. & Anderson, C. 2011. *Gwyddion - Free SPM data analysis software; v. 2.25*.
- Knotek, P., Arsova, D., Vateva, E. & Tichy, L. 2009. Photo-expansion in Ge-As-S amorphous film monitored by digital holographic microscopy and atomic force microscopy. *J. Optoelectron. Adv. M.*, 11, 391-394.
- Knotek, P., Kincl, M., Tichy, L., Arsova, D., Ivanova, Z. G. & Ticha, H. 2010. Oxygen assisted photoinduced changes in $\text{Ge}_{39}\text{Ga}_2\text{S}_{59}$ amorphous thin film. *J. Non-Cryst. Solids*, 356, 2850-2857.
- Knotek, P. & Tichy, L. 2012. On photo-expansion and microlens formation in $(\text{GeS}_2)_{0.74}(\text{Sb}_2\text{S}_3)_{0.26}$ chalcogenide glass. *Mater. Res. Bull.*, 47, 4246-4251.
- Knotek, P., Vlcek, M., Kincl, M. & Tichy, L. 2012. On the ultraviolet light induced oxidation of amorphous As_2S_3 film. *Thin Solid Films*, 520, 5472-5478.
- Lim, C. S., Hong, M. H., Kumar, A. S., Rahman, M. & Liu, X. D. 2006. Fabrication of concave micro lens array using laser patterning and isotropic etching. *Int. J. Mach. Tool Manu.*, 46, 552-558.
- Lin, C. G., Li, Z. B., Ying, L., Xu, Y. S., Zhang, P. Q., Dai, S. X., Xu, T. F. & Nie, Q. H. 2012. Network Structure in $\text{GeS}_2\text{-Sb}_2\text{S}_3$ Chalcogenide Glasses: Raman Spectroscopy and Phase Transformation Study. *J. Phys. Chem. C*, 116, 5862-5867.

- Marquez, E., Jimenez-Garay, R. & Gonzalez-Leal, J. M. 2009. Light-induced changes in the structure and optical dispersion and absorption of amorphous $\text{As}_{40}\text{S}_{20}\text{Se}_{40}$ thin films. *Mater. Chem. Phys.*, 115, 751-756.
- Mendes, M. 2006. Semiconductor applications using short-pulsed UV lasers. *Solid State Technol.*, 49, 42-46.
- Messaddeq, S. H., Siu LI, M., Lezal, D., Ribeiro, S. J. L. & Messaddeq, Y. 2001. Above bandgap induced photoexpansion and photobleaching in Ga-Ge-S based glasses. *J. Non-Cryst. Solids*, 284, 282-287.
- Phillips, J. C. 1979. Topology of covalent non-crystalline solids 1- short-range order in chalcogenide alloys. *J. Non-Cryst. Solids*, 34, 153-181.

